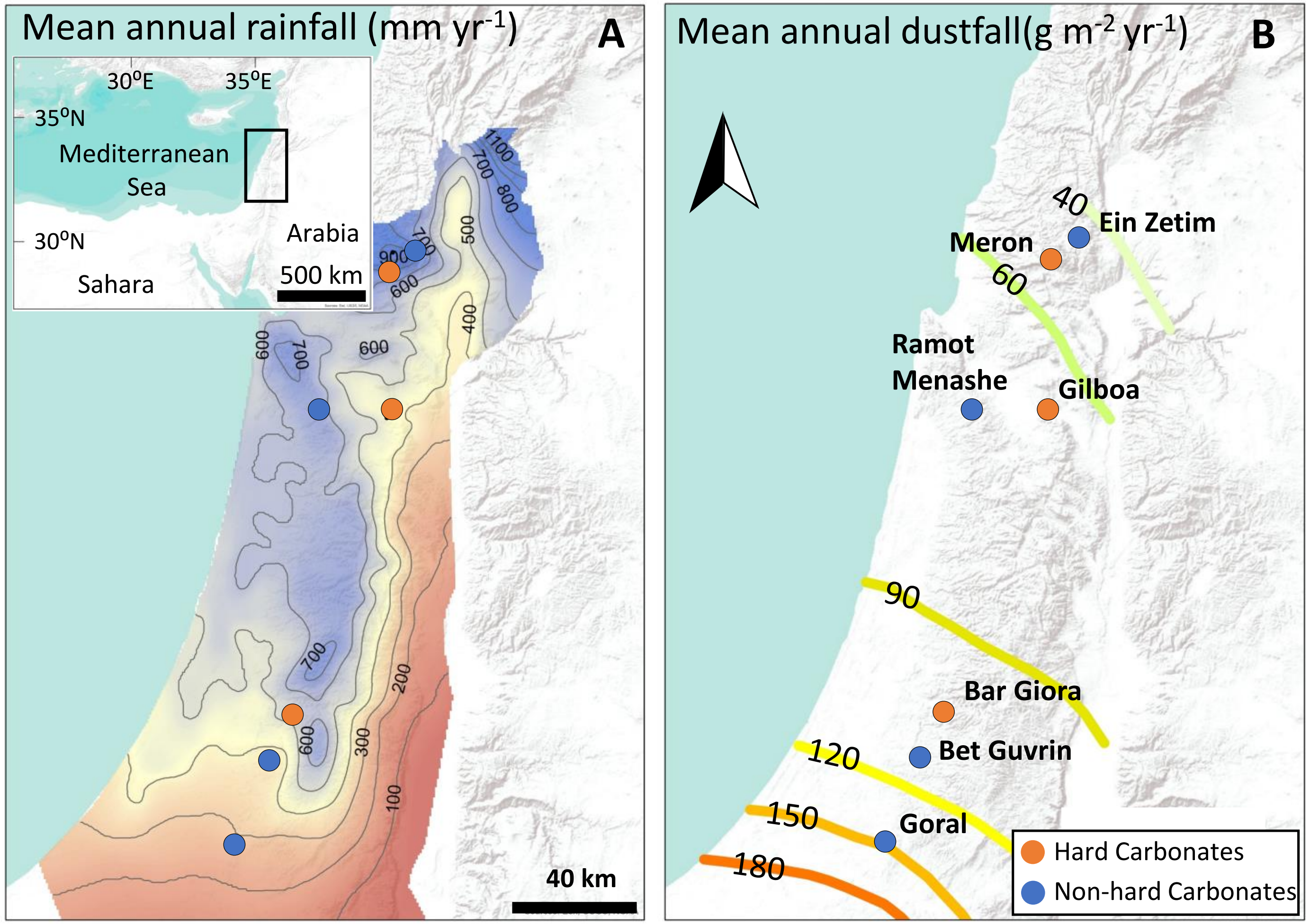

Location map of the study sites in the Eastern Mediterranean. A) Mean annual rainfall (mm) based on data from the Israel Meteorological service (http://www.ims.gov.il). Study sites symbols delineate soft chalk (blue circles), hard dolo-limestone (orange circles) and cinder cones (red triangles). Note the prominent climatic gradient. B) Mean annual current dust deposition rates (g m^{-2}) based on Ganor (1975) and Ganor and Foner (1996).

Table 1: Study sites, regolith dust fraction and chemical depletion data

Study site	Lithology	Mean annual rainfall[c]	Dust deposition rate[a]	Elevation	*CDF*[b]	f_d[b]	Clasts %	Soil depth
		(mm)	(g m^{-2} yr^{-1})	(m)				(cm)
Goral Hills (GOR)	Chalk	250	150	380	0.04	0.52	36%	32
Bet Guvrin (BGV)	Chalk	400	120	390	0.23	0.70	26%	14
Ramot Menashe (RAM)	Chalk & chert	650	70	210	0.45	0.17	31%	15
En Zetim (ZET)	Chalk	800	55	790	0.15	0.13	32%	37
Gilboa (GLB)	Dolo-limestone	450	70	320	0.51	0.44	30%	37
Bar Giora (BRG)	Dolo-limestone	550	100	510	0.55	0.45	30%	45
Meron (MER)	Dolo-limestone	900	45	900	0.45	0.14	46%	5

a. Modern deposition rates based on Ganor (1975) and Ganor and Foner (1996).

b. Weight fraction of bulk regolith. Calculated from concentrations of immobile elements (Ben-Asher et al., 2019).

c. Israel Meteorological Service. http://www.ims.gov.il

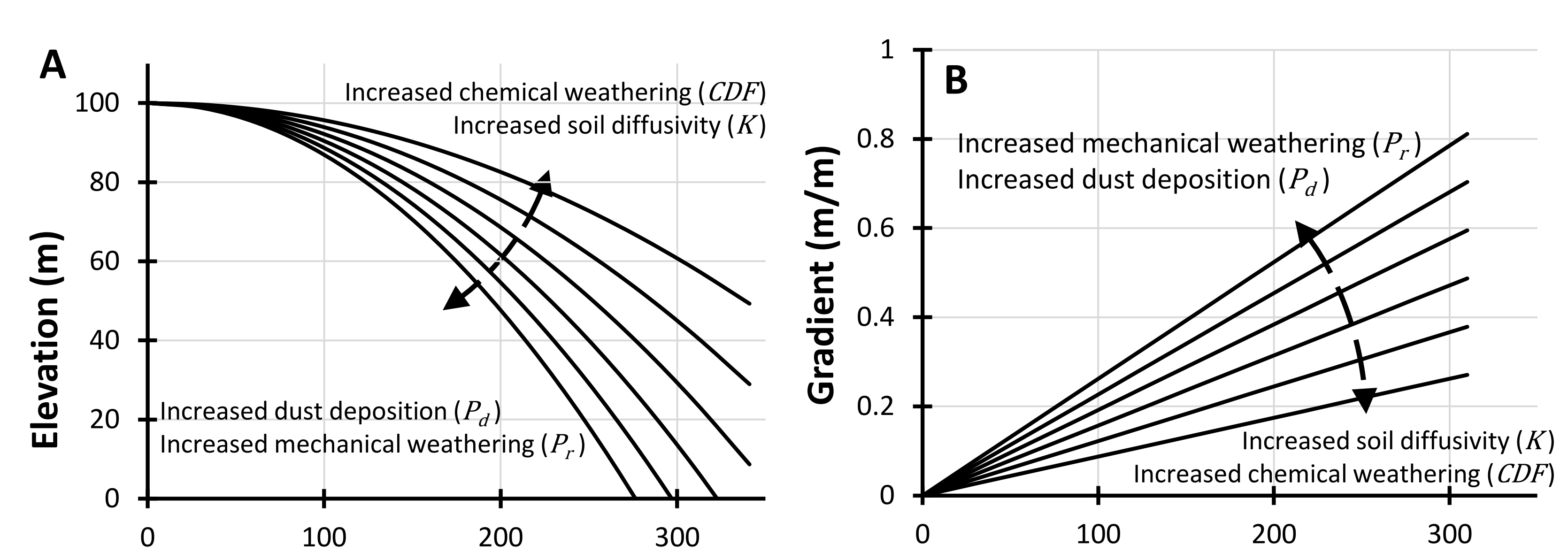

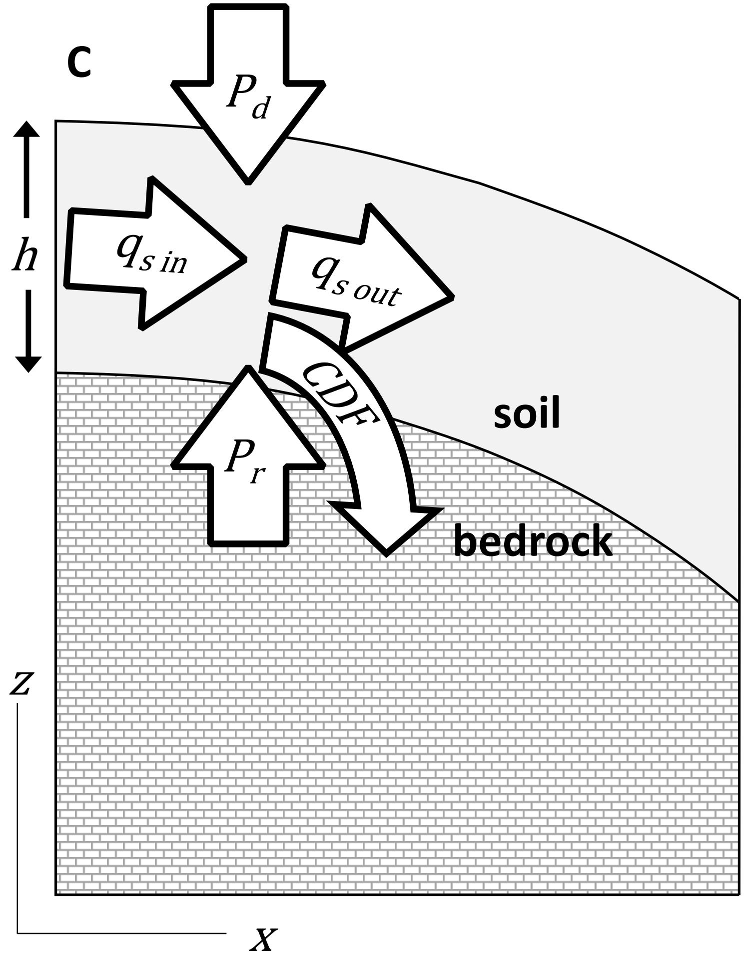

A) Theoretical hillslope profiles as a function of the distance from divide (1D profile) under steady state conditions where soil flux is linear with hillslope gradient. The predicted profiles are parabolic in form. Note the expected influence of key parameters (P_d and *CDF*) on hillslope curvature. B) Hillslope gradient as a function of the distance from the divide under the scenarios depicted in A. Note the linear dependency between hillslope gradient and the distance from the divide and the expected influence of key parameters on the slope of this line (i.e. hillslope curvature). C) A modified soil mass balance formulation along a hillslope element including soil influx and outflux (q_s), soil production from mechanical weathering of bedrock (P_r), dust deposition rate (P_d) and a chemical depletion fraction (*CDF*).

$$\nabla^2 z = \frac{(P_r + P_d)(1 - CDF)}{\rho_s K}$$

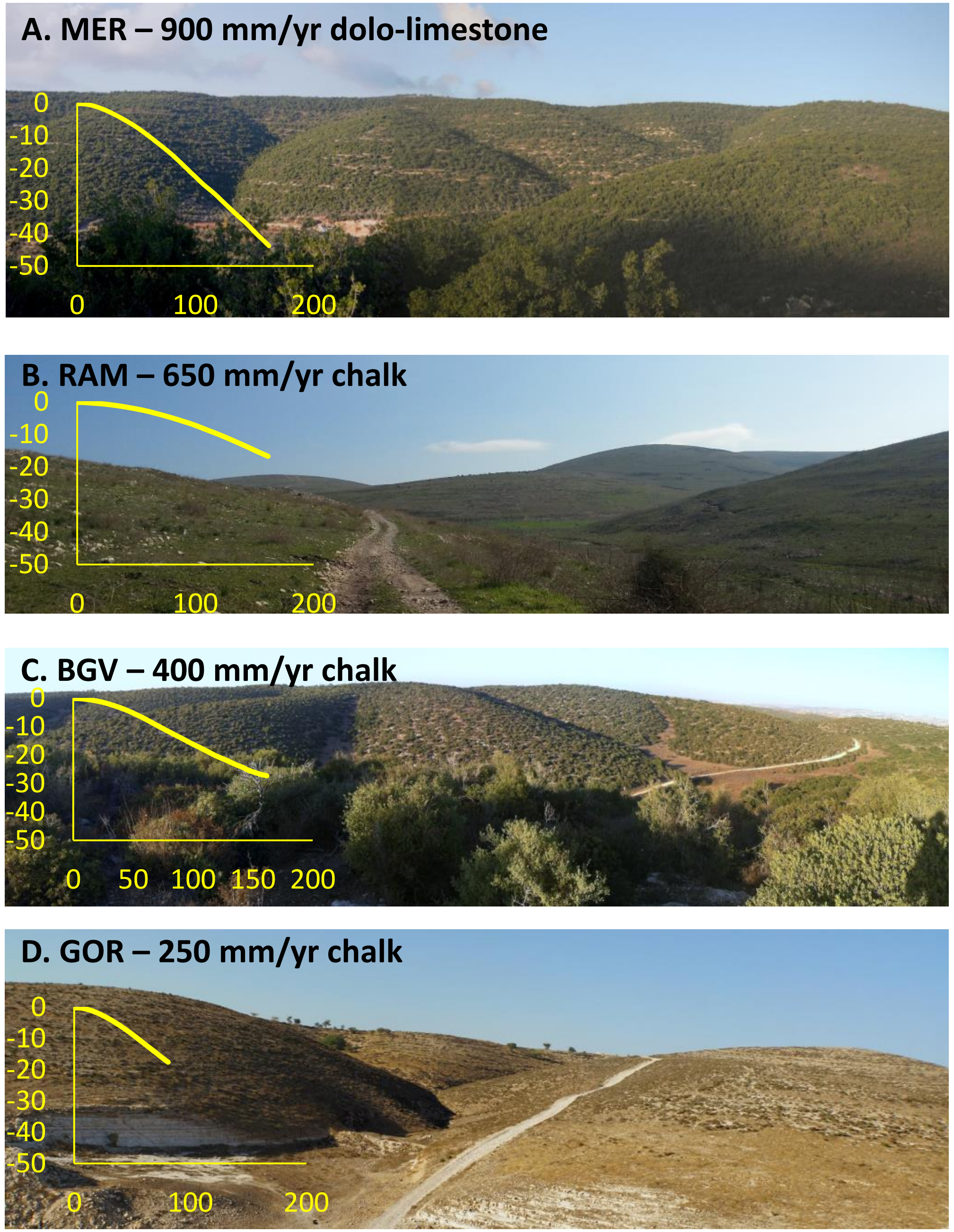

Characteristic morphology of several study sites located along a climatic gradient. Yellow subplot shows averaged elevation vs. distance profile from high resolution data. Note the prominent hillslope convexity and the variability between study sites. A) Meron mountain range (MER), rainfall: 900 mm yr^{-1}. B) Ramot Menashe highlands (RAM), rainfall: 650 mm yr^{-1}. C) Bet Guvrin hills (BGV), rainfall: 400 mm yr^{-1}. D) Goral Hills (GOR), rainfall: 250 mm yr^{-1}).

A) ^{36}Cl-derived hilltop denudation rates (mm/kyr) vs. mean annual rainfall (mm). Blue symbols: study sites with non-durable rocks (chalk). Orange symbols: study sites of hard carbonate. Note the prominent increase in denudation rate with precipitation. Note also that non-durable carbonates erode faster than hard carbonates for a given annual rainfall. B) Comparison with previous studies. Blue and orange lines delineate the maximum potential dissolution rate (Eq. 12: White, 1984) of hard (~2.7 g cm^{-3}) and soft carbonates (~1.8 g cm^{-3}), respectively. Note that the total denudation at some sites exceed the potential dissolution rate and must include mechanical weathering. Comparison with previous studies highlight that MER and ZET sites are characterized by uncommonly high rates and that soft carbonates erode faster than hard carbonates.

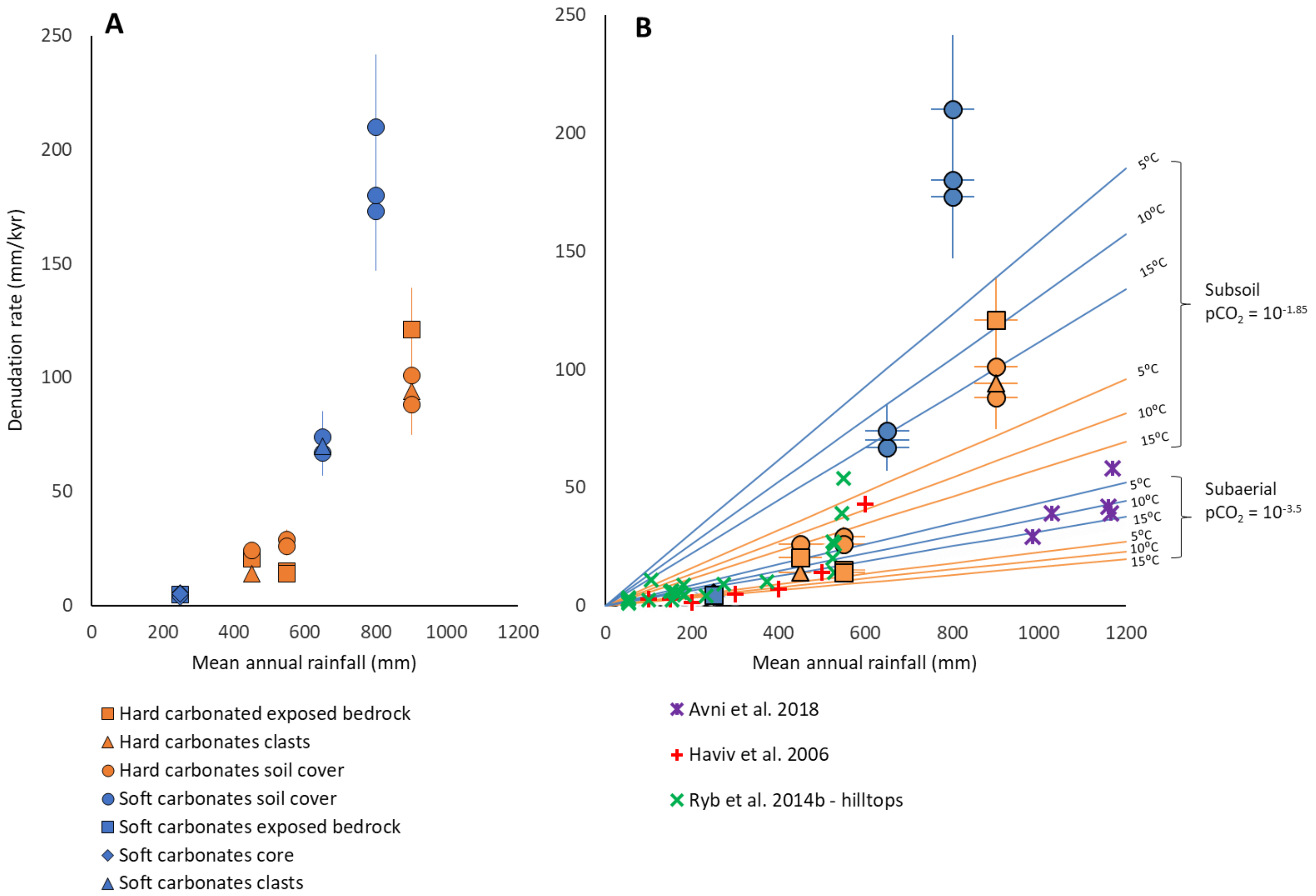

Observed hilltop curvature vs. the mean annual rainfall. Note how hilltop curvature decreases across the semi-arid to sub-humid transition (250-650 mm/yr) where dust flux decreases, and chemical depletion increases. In the wetter region (650–900 mm/yr) where dust flux and chemical depletion are quasi uniform the trend in the curvature mimics the denudation rate pattern.

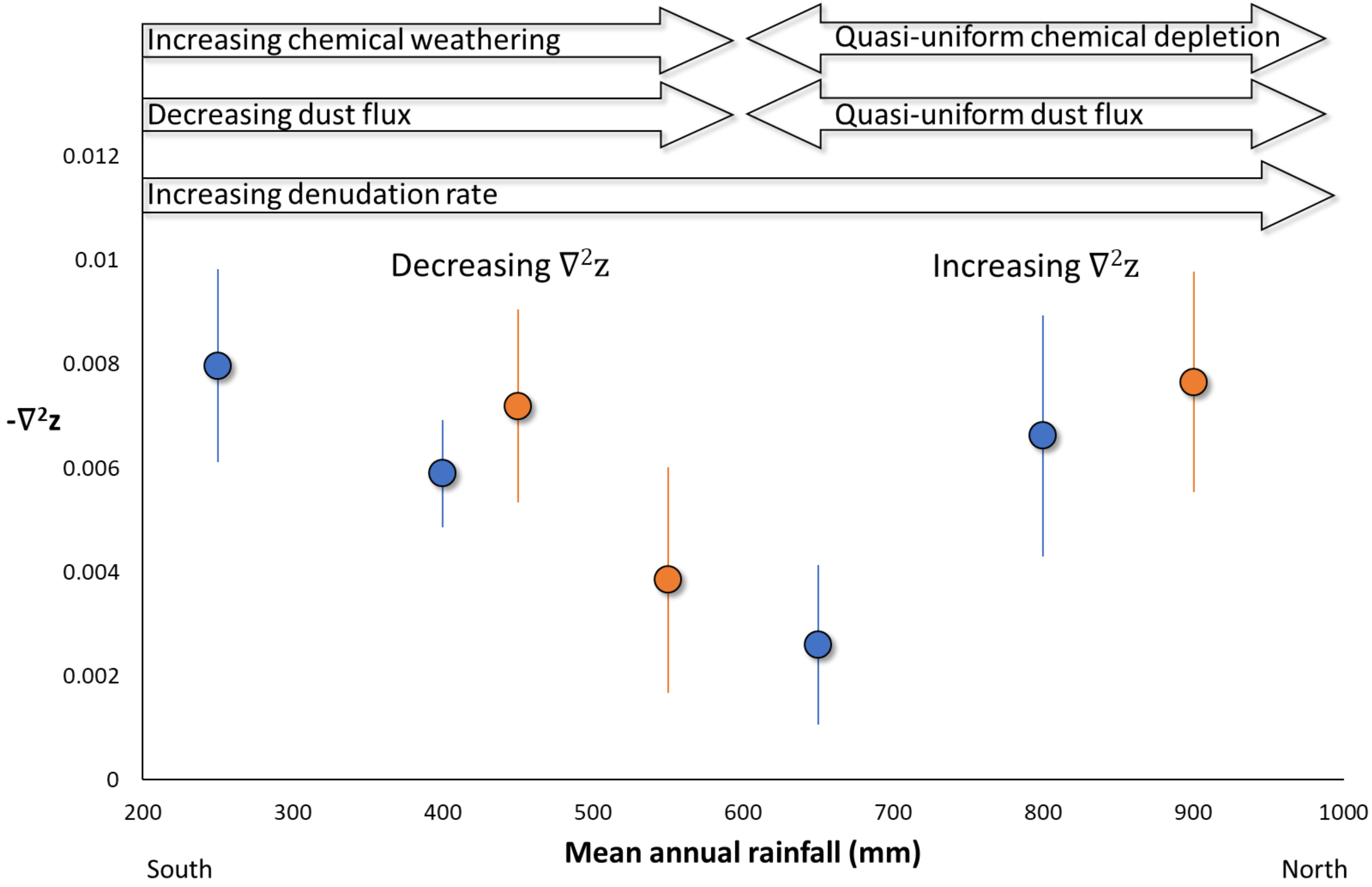

Observed (black circles) vs. predicted (white) hilltop curvature. The predicted hilltop curvature (see equation below) is based on data derived from immobile elements (*CDF, f_d*), ^{36}Cl (P_r), numerical modelling (K) and the density of bedrock and regolith (ρ_s, ρ_r). The observed curvature errors represent the spatial variability in hilltop curvature (see the methods section for more information). The calculated curvature in BGV site is based on the denudation rate in the nearby GOR site. The two sites are located only 30 km apart and composed of similar geologic unit of marine Eocene chalk (Avni and Sneh, 2008; Hirsch, 1983). Both sites also share similar elevation of 300-450 m a.s.l and situated in similar tectonic settings, at the higher western foothills ('Higher Shefela') of the Hevron anticline (Bar et al., 2016).

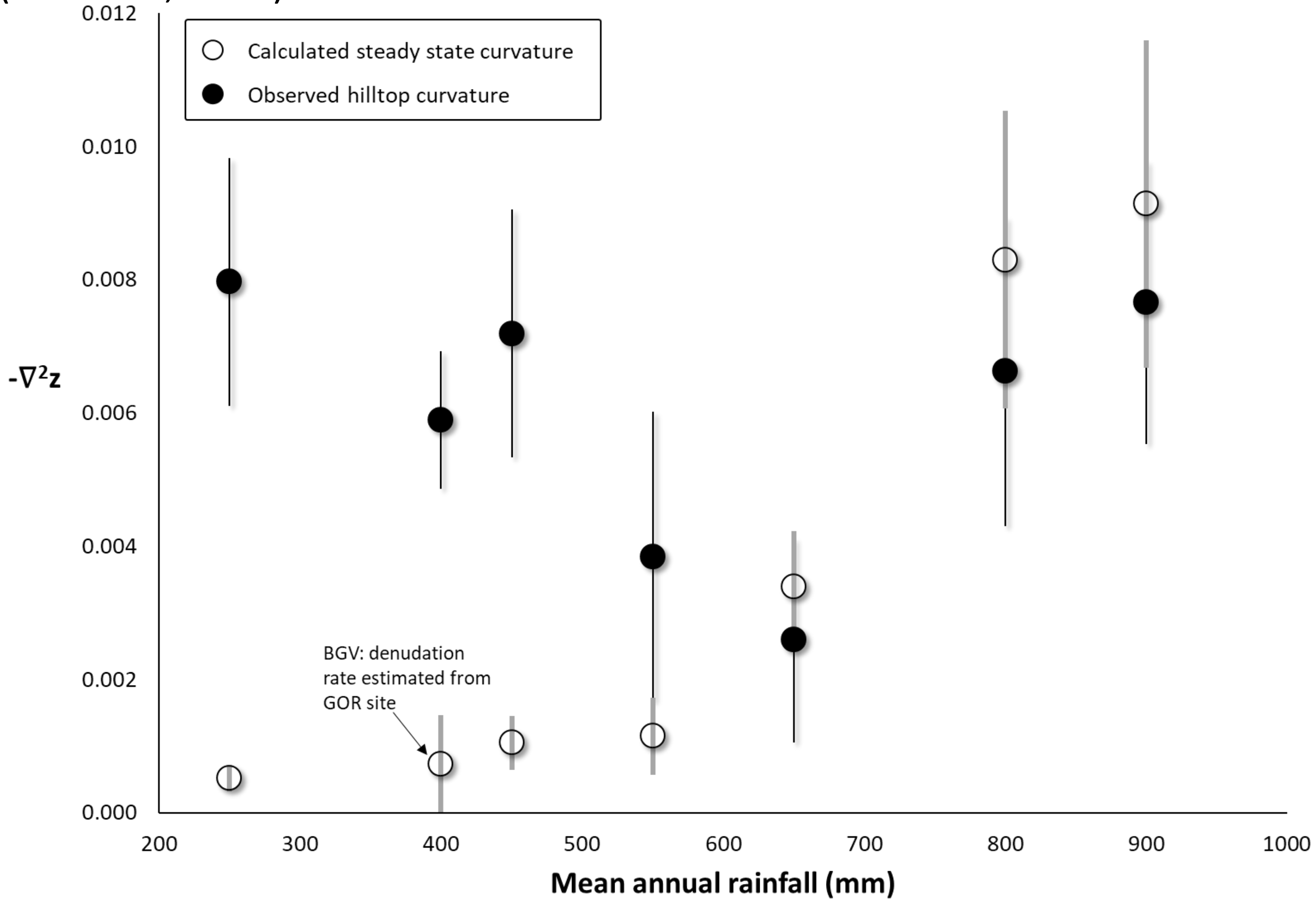

$$\nabla^2 z = \frac{(P_r + P_d)(1 - CDF)}{\rho_s K}$$